EPR study of spin dynamics near the percolation threshold of $Rb_2Mn_cMg_{1-c}F_4$

W. M. Walsh, Jr.
Bell Laboratories, Murray Hill, New Jersey 07974

R. J. Birgeneau
Department of Physics and Center for Materials Science and Engineering, Massachusetts Institute of Technology, Cambridge, Massachusetts 02139

L. W. Rupp, Jr., and H. J. Guggenheim
Bell Laboratories, Murray Hill, New Jersey 07974
(Received 18 June 1979)

Electron-paramagnetic-resonance studies of the dilute two-dimensional antiferromagnet $Rb_2Mn_cMg_{1-c}F_4$ are reported versus both concentration and temperature. Particular attention has been paid to the temperature-dependent resonance linewidth near the percolatiton threshold, $c \simeq c_p = 0.59$, where a variety of interesting effects are observed: At high temperatures the linewidth is dominated by the long-time, $q \to 0$ diffusive part of the dipolar interaction having $(3\cos^2\theta - 1)^2$ anisotropy characteristic of two-dimensional systems. This contribution increases rapidly below the percolation concentration due to slowing of spin diffusion as the spin network breaks up into finite clusters. For $T < 30$ K and $c \sim c_p$ the linewidth is dominated by antiferromagnetic correlation effects leading to rapid line broadening as T decreases and a change of anisotropy. Both effects are only crudely described by the RPA theory. For $c < c_p$ most of the resonance intensity remains centered at $g = 2$ down to the lowest temperatures reflecting the absence of long-range order. Near and above c_p and for $T < 4.2$ K some intensity is shifted to lower fields, however, as the percolation cluster orders. Most remarkable is the appearance of a nine-line superstructure on the $g = 2$ resonance at 1.6 K in samples near the percolation concentration. This illustrates the critical slowing of spin dynamics on a time scale of 10^{-9} sec and is believed to be the resonance of spins surrounded by nonmagnetic nearest neighbors but coupled to next-nearest-neighbor spins, most of which are locked to clusters. Evidence of anisotropic spin fluctuations and the possibility of reduced next-nearest-neighbor exchange or very large zero-point spin deviation is found in this regime.

I. INTRODUCTION

In the past few years a variety of interesting developments have occurred regarding percolation phenomena in insulating magnets. In particular it has been shown that certain antiferromagnetic systems such as $Rb_2Mn_cMg_{1-c}F_4$ and $Mn_cZn_{1-c}F_2$ show well-defined percolation transitions as functions of concentration c.[1,2] The percolation effect manifests itself as a continuous diminution of the Néel temperature, T_N, as a function of concentration until, for $c = c_p$, one has $T_N = 0$ K. For $c \leq c_p$ no long-range order occurs. Somewhat suprisingly, in the transition-metal fluorides studied to date, c_p corresponds closely, if not exactly, to that anticipated on the basis of nearest-neighbor interactions alone. In critical-phenomena language, the phase transitions in the diluted systems with $c_p < c < 1$ correspond to a line of second-order transitions which terminates at the percolation multicritical point at $T = 0$, $c = c_p$. The static and dynamic behavior around this new type of multicritical point is both very rich and quite subtle. The most detailed experimental studies of such systems to date have been primarily via neutron scattering[1,2] and by "computer experiment" techniques.[3,4]

Recent developments, particularly in lower-dimensional systems, have shown that electron paramagnetic resonance (EPR) experiments may provide detailed information about the spin dynamics in concentrated magnetic systems. In particular, a thorough theoretical and experimental EPR study of the two-dimensional (2-D) antiferromagnet K_2MnF_4 has been made by Richards and Salamon.[5] They have shown that by measuring both the temperature dependence and the angular variation of the resonance width one can obtain information about both long-wavelength diffusive processes at high temperatures and short-wavelength antiferromagnetic correlation effects in the precritical region in two dimensions. Both of these are of considerable interest in the percolation problem.

In this paper we report a detailed EPR study of the model 2-D percolation system $Rb_2Mn_cMg_{1-c}F_4$.

Many aspects of this system have already been studied experimentally using neutron scattering techniques[1]; in addition, Harris and Kirkpatrick[4] have made a theoretical study of the low-temperature thermodynamic and dynamic behavior near percolation. $Rb_2Mn_cMg_{1-c}F_4$ has the very attractive features that (a) the Hamiltonian is simple and well characterized, (b) the system is known to have a well-defined percolation transition for $c \simeq c_p = 0.59$,[1] and (c) from the neutron scattering studies rather complete information on the temperature-dependent static correlations for $c \simeq c_p$ is available. The spirit of the present work is primarily empirical. In particular, we wished to explore the usefulness of EPR for characterizing percolation effects in insulating magnets. As we shall show, in two dimensions there are indeed a variety of dramatic effects which either give or promise to give detailed information about percolation; these experiments thus serve to establish EPR as an important experimental probe of dilute magnets, especially for $c \simeq c_p$. We observe novel behavior in the resonance signal for $c \simeq c_p$ and $T < 4.2$ K which we associate with a freezing of the cluster spin motion, analogous to critical slowing down at ordinary phase transitions. In this case EPR yields dynamical information on an energy scale rather finer than that obtainable using ordinary neutron scattering techniques. Takano and Yokozawa[6] have reported a room-temperature EPR study of $K_2Mn_cMg_{1-c}F_4$ which is generally consistent with our results for high temperatures.

The format of this paper is as follows. In Sec. II we give general background information including a summary of our current picture of percolation in $Rb_2Mn_cMg_{1-c}F_4$; in addition we review the theory of EPR in 2-D near-Heisenberg antiferromagnets. Section III describes the experimental results while Sec. IV contains a discussion of the results. We make a few final remarks in Sec. V.

II. GENERAL BACKGROUND

A. Percolation in $Rb_2Mn_cMg_{1-c}F_4$

The crystal structure of Rb_2MnF_4 is shown in Fig. 1. The magnetic properties of this material have been investigated by a wide variety of techniques and indeed it is now one of the best understood magnetic systems. The spin Hamiltonian may, to a very good approximation, be written

$$H = J_1 \sum_{\langle nn \rangle} \vec{S}_i \cdot \vec{S}_j + J_2 \sum_{\langle nnn \rangle} \vec{S}_i \cdot \vec{S}_j + \sum_{r>j} \frac{g^2 \mu_B^2}{r_{ij}^3} [\vec{S}_i \cdot \vec{S}_j - 3(\vec{S}_i \cdot \hat{r}_{ij})(\vec{S}_j \cdot \hat{r}_{ij})] \ , \quad (1)$$

with $J_1 = 0.653$ meV, $J_2 = 0.012$ meV, $g = 2.00$, and $S = \frac{5}{2}$; in pure Rb_2MnF_4 at 5 K, $r_{nn} = 4.215$ Å while

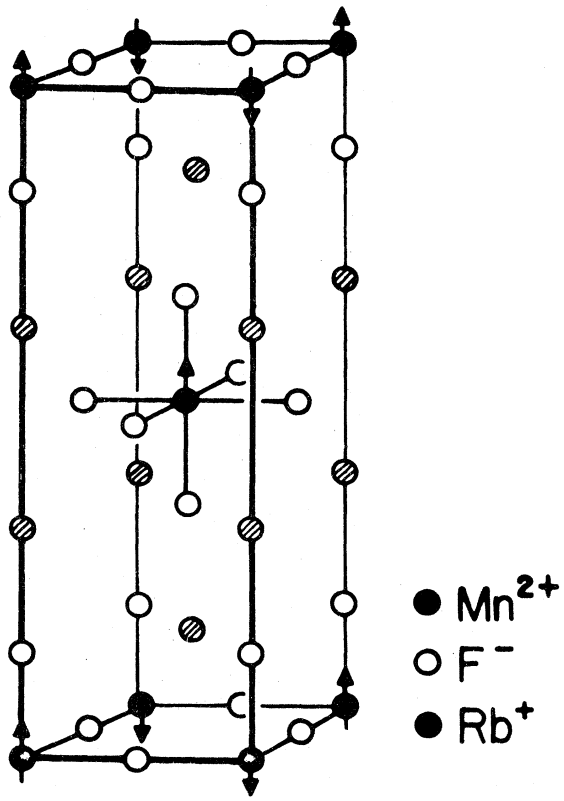

FIG. 1. Crystal structure and antiferromagnetic order of Rb_2MnF_4.

in $Rb_2Mn_{0.57}Mg_{0.43}F_4$, $r_{nn} = 4.150$ Å.[7] Here J_1 and J_2 are the nearest-neighbor (nn) and next-nearest-neighbor (nnn) in-plane exchange interactions, respectively. More distant neighbor in-plane exchange couplings as well as the between-plane interactions are negligible. In the concentrated material, the dipolar interaction is often represented as an anisotropy field term $H = -g\mu_B H_A \sum_i (-)^i S_i^z$ with $g\mu_B H_a = 0.032$ meV and the Z axis perpendicular to the planes. As discussed by a variety of authors, the negligible between-plane interaction together with the symmetry of the ordered antiferromagnetic (AF) structure lead to almost ideal 2-D behavior in this system.[8]

Dilution of Rb_2MnF_4 by substitution of nonmagnetic Mg^{2+} ions for Mn^{2+} is readily accomplished as described below. The resulting alloys appear to be nearly perfectly random on a microscopic scale and display the percolation behavior expected on the basis of nearest-neighbor coupling. Below the critical concentration $c_p = 0.59$ only finite islands or clusters of nearest-neighbor Mn^{2+} ions will occur. Figure 2 is a computer generated 100×100 array at c_p occupancy with the percolation cluster identified by antiferromagnetic order, as would ideally occur at $T = 0$ K. The rapid nature of the phase transition in concentra-

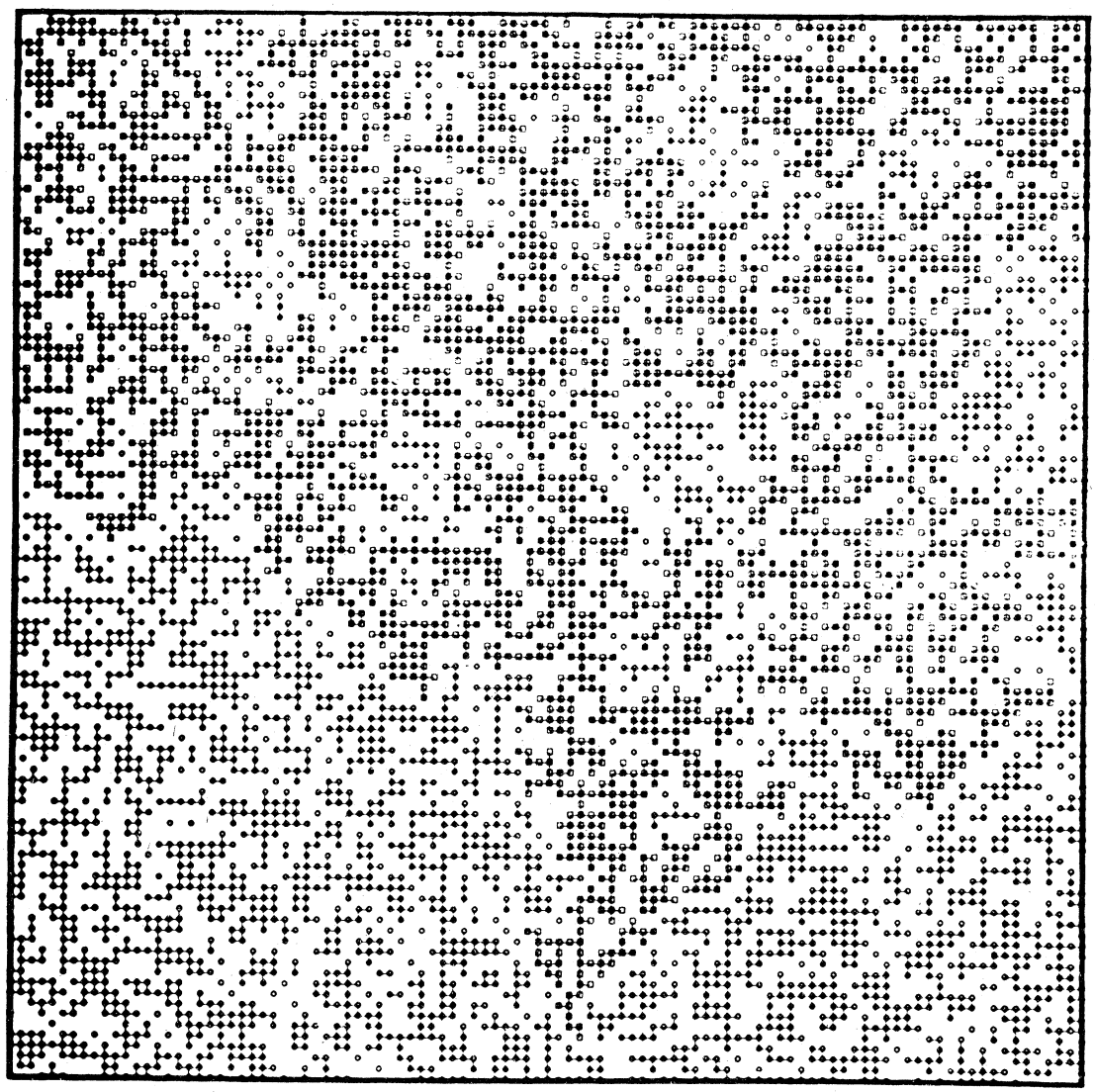

FIG. 2. Random occupancy of the 2-D square lattice at the percolation concentration, $c = 0.59$. The percolation cluster is indicated by solid and open squares representing the AF nearest-neighbor coupling. This 100×100 array was taken within a calculated 140×140 array to minimize edge errors in the percolation cluster.

tion is illustrated in Fig. 3 where we show the fraction of occupied sites in the infinite network as a function of concentration; near c_p one has $P(c)/c \sim (c-0.593)^{0.14}$. We also show for some computer-generated 100×100 arrays the mean fraction of sites belonging to the finite clusters. Different clusters may be coupled by the very weak nnn exchange; however this nnn exchange is antiferromagnetic and thus it is not supportive of the long-range-ordered (LRO) state of the pure material. Hence for $c < 0.59$ no simple LRO state can occur.

As we noted in the Introduction the system $Rb_2Mn_cMg_{1-c}F_4$ for $c \simeq c_p$ has been extensively studied using neutron scattering techniques; these experiments have indeed demonstrated that the Néel temperature becomes less than 1 K (T_N for Rb_2MnF_4 is 38.4 K) for $c < 0.59$ as anticipated on the basis of the nn percolation model. The point $T_N = 0$, $c = c_p$ may then be described as a multicritical point terminating the line of AF second-order transitions of the infinitely connected network for $c > c_p$. The results of Birgeneau *et al.*[1] for the static inverse correlation length as a function of temperature for $c = 0.54$ and $c = 0.57$ are shown in Fig. 4. These data represent an average of the longitudinal (that is parallel to the spin anisotropy axis which in turn is perpendicular to the planes) and transverse inverse lengths. These results show the essential features of the percolation effects. Below about 30 K the nn AF correlations within the clusters begin to establish

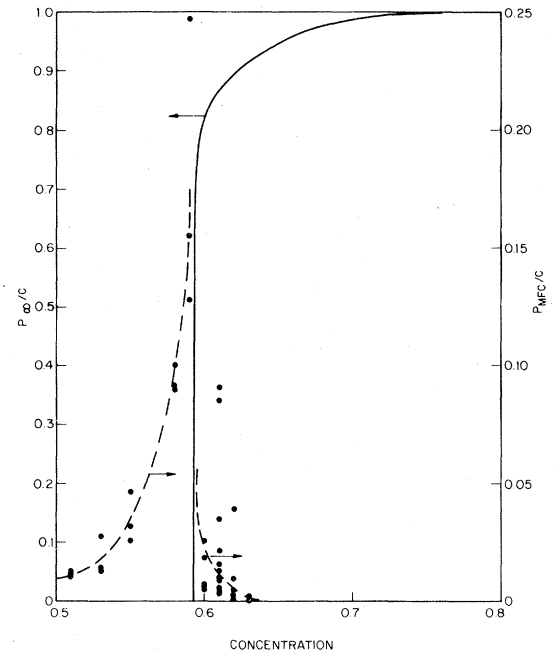

FIG. 3. Percolation transition of the 2-D square lattice illustrated by the fractional occupancy of the *infinite* cluster P_∞/c for $c > c_p = 0.593$ [solid curve, left-hand scale; S. Kirkpatrick (private communication)]. The fractional mean-*finite*-cluster size P_{MFC}/c computed for a number of 100×100 arrays is also shown (dashed curves, right-hand scale).

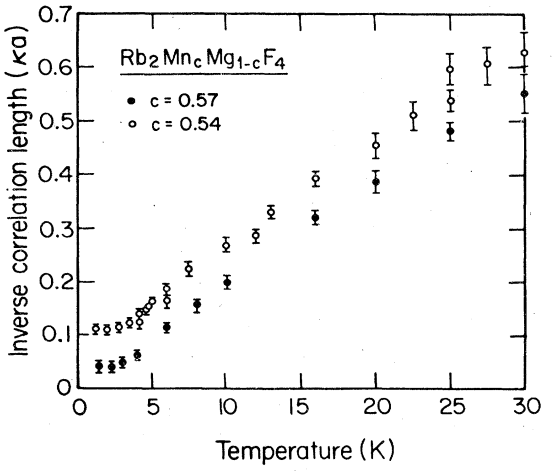

FIG. 4. Static inverse correlation length vs temperature for $Rb_2Mn_cMg_{1-c}F_4$ at $c = 0.54$ and 0.57 (from Ref. 1). The degree of order increases rapidly with decreasing temperature and increasing concentration but saturates at the finite cluster size available in the prepercolation regime.

themselves. The correlation length grows with decreasing temperature until about 4 K at which point it equals the size of the clusters so that no further increase can occur. More detailed neutron experiments[9] suggest that below 4 K the spins are essentially oriented along the Z axis and that, with an energy resolution of about 0.1 meV, the clusters are static. As we shall show later, this "freezing" of the clusters manifests itself dramatically in the EPR spectra; this, in turn, means that EPR provides an excellent probe of the cluster spin dynamics at very low energies.

As noted above, our essential aim in this study was to document experimentally the manner in which percolation effects manifest themselves in EPR spectra. Before describing our results we will, therefore, first review the theory of EPR linewidths in concentrated systems.

B. EPR linewidths in concentrated systems

In this subsection we lean strongly on the paper of Richards and Salamon describing the theory and experimental study of EPR linewidths in 2-D antiferromagnets[5]; the reader is referred to that paper for a full discussion. It is convenient to consider the system separately at very high and at low temperatures.

As is well known, in 3-D concentrated magnetic systems at high temperatures the EPR linewidth in frequency units is given by

$$\Delta\omega \simeq \omega_p^2/\omega_e \ , \tag{2}$$

where ω_p is the rms dipolar perturbation frequency and ω_e is the exchange frequency [cf. Eq. (2)]. This result, in turn, requires that the power spectrum

$$P(\omega) = \int_{-\infty}^{\infty} dt \ \langle \omega_p(t)\omega_p(0)\rangle e^{i\omega t} \tag{3}$$

be finite at $\omega = 0$. Richards and Salamon, however, have emphasized that in two dimensions the long-time correlations are dominated by spin diffusion so that

$$\lim_{t\to\infty} \langle \omega_p(t)\omega_p(0)\rangle \propto |t|^{-1} \ , \tag{4}$$

giving rise to a logarithmic divergence in the power spectrum as $\omega \to 0$. This then leads to an extra contribution to the linewidth from the spin diffusion. Further, this extra component has the geometry of the secular part of the dipole-dipole interaction with $q \to 0$. This means that for a two-dimensional lattice the spin-diffusion-generated term has the simple angular dependence $(3\cos^2\theta - 1)^2$, where θ is the angle between the applied field $\vec{H}$ and the normal to the plane. By contrast, the conventional exchange narrowing term, Eq. (2), which in the RPA involves the square of a two-spin correlation function times a dipolar factor averaged over the whole Brillouin zone, varies only weakly with θ. To a good approximation

in two dimensions the EPR linewidth at high temperatures should have an angular dependence

$$\Delta H = \alpha + \beta(3\cos^2\theta - 1)^2 \ , \tag{5}$$

where α represents the contribution from the $q \neq 0$ exchange narrowing and where the β term measures explicitly the contributions of processes from the $q \sim 0$ region of the Brillouin zone. As emphasized by Richards and Salamon, this correlation between the EPR linewidth and spin-spin correlations in specific regions of the Brillouin zone greatly enhances the power of EPR as a probe of the AF spin fluctuations in two-dimensional systems. The general applicability of the above ideas and specifically Eq. (5) has been confirmed in detail experimentally in K_2MnF_4.[5]

The two linewidth contributions also exhibit distinct behavior as the temperature is reduced: Both α and β involve a factor $\chi_0 T$ in their denominators and the square of a two-spin correlation function times a dipolar factor in their numerators. When averaged over the Brillouin zone the numerator is only weakly temperature dependent in the case of α but the singular behavior of β near $q \sim 0$ leads, via the fluctuation-dissipation theorem, to a $(\chi_0 T)^2$ contribution.[5] Thus one may anticipate $\alpha \sim (\chi_0 T)^{-1}$ and $\beta \sim \chi_0 T$ where

$$\chi_0 T = \tfrac{1}{3} g^2 \mu_B^2 S(S+1) \frac{T}{T+\Theta} \ , \tag{6}$$

for

$$T >> \Theta \sim \tfrac{4}{3}(J_1/k_B) S(S+1) = 88 \text{ K}$$

in Rb_2MnF_4. With decreasing temperature it is therefore expected that α may increase whereas β should decrease.

At still lower temperatures the spin-spin correlations must reflect the short-range antiferromagnetic coupling which causes a rapid increase in the wave-vector-dependent susceptibility at the AF superlattice position $\vec{K}_0 = (\frac{1}{2}a^*, \frac{1}{2}a^*)$, where a^* is a reciprocal-lattice vector of the 2-D Brillouin zone. This regime is seen in Fig. 4 for $T < 30$ K as AF ordering of limited range sets in even in material diluted below the percolation threshold. As the spin correlations $\langle \vec{S}(\vec{K}_0, 0) \cdot \vec{S}(\vec{K}_0, 0) \rangle$ grow a new contribution to the ESR linewidth appears with a distinct anisotropy $f(\theta)$ to be discussed below

$$\Delta H = \alpha(T) + \beta(T)(3\cos^2\theta - 1)^2 + \gamma(T) f(\theta) \ . \tag{7}$$

The theory of $\gamma(T)$ has been given by Huber and Kawasaki[10–12] in the context of 3-D antiferromagnets; for completeness their results are summarized here. The fundamental quantity involved is the zero-field spin-spin relaxation time which, for Lorentzian lines, may be written

$$\frac{1}{T_2^\alpha} \sim \frac{1}{\langle S^\alpha S^\alpha \rangle} \int_0^\infty dt \, (\dot{S}^\alpha(t), \dot{S}^\alpha(0)) \ , \tag{8}$$

where $S^\alpha = g\mu_B \sum_i S_i^\alpha$, $\dot{S} = (i/\hbar)[S, H]$, and (A, B) is a relaxation function.[11] The dipolar anisotropy tensor at $\vec{q} = \vec{K}_0$ has uniaxial symmetry ($D_{xx} = D_{yy} = D_\perp, D_{zz} = D_\parallel$) and varies little around $\vec{K}_0$.[12] If one assumes that the spin fluctuations are isotropic and if one makes the usual RPA factorization of the four-spin correlation functions[10,11] then one obtains

$$\left(\frac{1}{T_2^\theta}\right)_{\vec{q} \simeq \vec{K}_0} \sim \frac{c}{\langle S^\alpha S^\alpha \rangle} \left(D_\parallel - D_\perp\right)^2 \sin^2\theta \sum_{\vec{q} \simeq \vec{K}_0} \int_0^\infty dt \, \langle S\alpha(\vec{q}, t) S\alpha(\vec{q}, 0) \rangle^2 \ , \tag{9}$$

for spin fluctuations along a direction making an angle θ with respect to the Z axis. For strongly correlated spins we may write

$$\langle S^\alpha(\vec{q}^{\,*}, t) S^\alpha(\vec{q}^{\,*}, 0) \rangle = \frac{\kappa^\eta e^{-\Gamma(\vec{q}^{\,*})t}}{\kappa^2 + q^{*2}} \ , \tag{10}$$

where $\vec{q}^{\,*} = \vec{q} - \vec{K}_0$ and κ is the static inverse correlation length as shown for $Rb_2Mn_cMg_{1-c}F_4$ in Fig. 4. From dynamic scaling[13] we expect $\Gamma(\vec{q}^{\,*}) \sim \kappa^Z f(q^*/\kappa)$. Substitution in Eq. (9) then gives

$$\sum_{\vec{q}} \int dt \, \langle \ \rangle^2 \sim \kappa^{-(4-d-2\eta+Z)} \ . \tag{11}$$

To further evaluate $\gamma(T)$ we also assume χ_0 to be weakly temperature dependent so that $\langle S^\alpha S^\alpha \rangle \sim T$. In an EPR experiment, for $\Gamma(0)$ much greater than the microwave energy, ΔH is simply proportional to $1/T_2^\theta$ averaged over the plane perpendicular to $\vec{H}$. Thus we have finally

$$\gamma(T) f(\theta) = (B/T)(D_\parallel - D_\perp)^2 \kappa^{-(4-d-2\eta+Z)}(1 + \cos^2\theta) \ . \tag{12}$$

In the percolation multicritical theory[14] $\kappa \sim T^{\nu_p/\phi}$ for a Heisenberg system where ν_p is the correlation-length exponent for the pure percolation problem and ϕ is the concentration-temperature crossover exponent. Hence we finally have

$$\gamma(T) \propto T^{-\nu_p(4-d-2\eta+Z)/\phi - 1} \ . \tag{13}$$

This result holds in d dimensions for an isotropic system. In two dimensions $\nu_p = 1.35$ and $\eta = 0.20$. Various theories give $\phi = 1$, however, the experi-

ments shown in Fig. 4. suggest $\phi \sim 1.5$. The parameter Z is not known for the 2-D percolation problem but in the pure system dynamic scaling gives $Z = 1$, a result we assume carries over to the percolation regime in making an estimate of the exponent in $\gamma(T)$. Thus the simple theory gives

$$\gamma(T) \propto T^{-3.5/\phi-1}$$

for a 2-D Heisenberg system with very weak uniaxial anisotropy. Thus $\gamma(T)$ should grow very rapidly with decreasing temperature.

We should emphasize that the theory outlined above applies only to the regime where the dipolar anisotropy has negligible influence on both the isotropy and the temperature dependence of the static correlations. In fact, we know from the neutron scattering measurements and from recent theory that the anisotropy is anomalously important in magnetic correlations in the percolation regime. Explicitly for $T \lesssim 10$ K it causes $\langle S^{\parallel}(-\vec{K}_0) S^{\parallel}(\vec{K}_0)\rangle$ to grow exponentially in T^{-1} while $\langle S^{\perp}(-\vec{K}_0) S^{\perp}(\vec{K}_0)\rangle$ saturates at a finite value. Thus the theory presented above must be regarded only as a qualitative estimate of the probable behavior both in regard to the temperature dependence and to the angular variation.

In summary then, EPR linewidths in two-dimensional near-Heisenberg antiferromagnets including those near the percolation concentration should have three separate components as exhibited in Eq. (7): (i) $\alpha(T)$, the conventional exchange-narrowed width, (ii) $\beta(T)(3\cos^2\theta-1)^2$, originating from $q \sim 0$ spin diffusion processes, and (iii) $\gamma(T) f(\theta)$, arising from antiferromagnetic critical correlations at $\vec{q} \simeq \vec{K}_0$. $\alpha(T)$ is expected to be weakly temperature dependent, $\beta(T)$ should dominate at high temperatures, and $\gamma(T)$ should dominate at low temperatures.

III. EXPERIMENTAL

A. Samples and apparatus

The samples used in the ESR studies were $\hat{c}$-plane platelets, typically $4 \times 4 \times 0.1$ mm, cleaved from single-crystal boules grown by the Czochralski method.[8] In several cases samples were taken from boules previously used in the neutron investigations.[1] The alloy samples were prepared from RbF, MnF_2, and MgF_2 crystalline material previously zone refined in an HF atmosphere. A 40 mol.% excess of RbF in the melt composition was found necessary to shift the phase equilibrium such that the desired Rb_2MF_4 phase would nucleate on a seed crystal harvested from an initial run. Under optimum conditions optically clear boules ~ 2 cm in diameter by ~ 4 cm long were obtained. The Mn to Mg composition ratio was found to vary by $\sim 4\%$ along the pulling ($\hat{c}$) axis, a variation of no importance for the very thin c-plane ESR samples, other than to introduce an uncertainty in the concentration. Weaker but significant radial concentration variations of $\sim 0.5\%$ were inferred from the ESR linewidth data obtained from several samples taken from a particular cleaved plate. Concentrations of Mn^{2+} from 10 to 70 at.% were studied with particular attention to the region $c \simeq c_p = 0.59$. Results for fully concentrated K_2MnF_4 are available in the literature.[5,6,15]

The experiments were performed at 12, 17.4, and 35 GHz using conventional homodyne bridge spectrometers. Usually magnetic field modulation was used to record absorption-derivative spectra. Absorption spectra were also recorded in cases of extremely wide resonance lines. Sensitivity was never a problem with such magnetically concentrated samples; to the contrary, sample volumes had usually to be minimized to avoid nonlinear spectrometer response due to excessive cavity loading on resonance. Samples were mounted on the side walls of dominant-mode rectangular cavities so that anisotropy studies from $\vec{H} \| \hat{c}$ to $\vec{H} \perp \hat{c}$ could be made by rotating the swept magnetic field in the horizontal plane. It was found necessary to space the samples away from the metallic cavity wall by mounting them on 0.125-mm fused-quartz plates: This minimized ESR line shape and position distortions which occur due to "image effects" when strong magnetic moments precess very near a highly conducting surface.

The temperature was controlled by electrical heating of the cavity which was thermally decoupled from a refrigerant bath by an evacuated brass can and stainless-steel waveguide. Cavity-wall temperature was measured and controlled by platinum- and carbon-resistor thermometers attached to the outside of the wall on which the sample was mounted. Temperature runs were made from 1.6 to ~ 20 K using liquid helium, from 15 to 100 K using liquid hydrogen and from 65 to 325 K using liquid nitrogen. A partial pressure of helium gas within the cavity served to equilibrate the sample temperature with that of the cavity wall but the fused-quartz spacer plate introduced enough thermal impedance between sample and wall to produce temperature differences of a few percent at the high end of each temperature range. These deviations were calibrated and corrected via runs made at fixed bath temperatures with He gas in both cavity and outer can to provide good thermal conduction.

B. Results

Here we will summarize the results of our extensive ESR studies versus angle, temperature, and magnetic concentration, postponing much of the discussion and interpretation to Sec. IV. At all but the lowest temperatures we observe a single, symmetrical resonance line centered on $g = 2$, as expected for

$Mn^{2+}(L=0, S=\frac{5}{2})$. The line shape is qualitatively Lorentzian, characteristic of exchange narrowing, but no effort has been made to examine subtle deviations from the Lorentzian form as was done previously.[5,6] All linewidths are peak-to-peak values taken from absorption-derivative spectra.

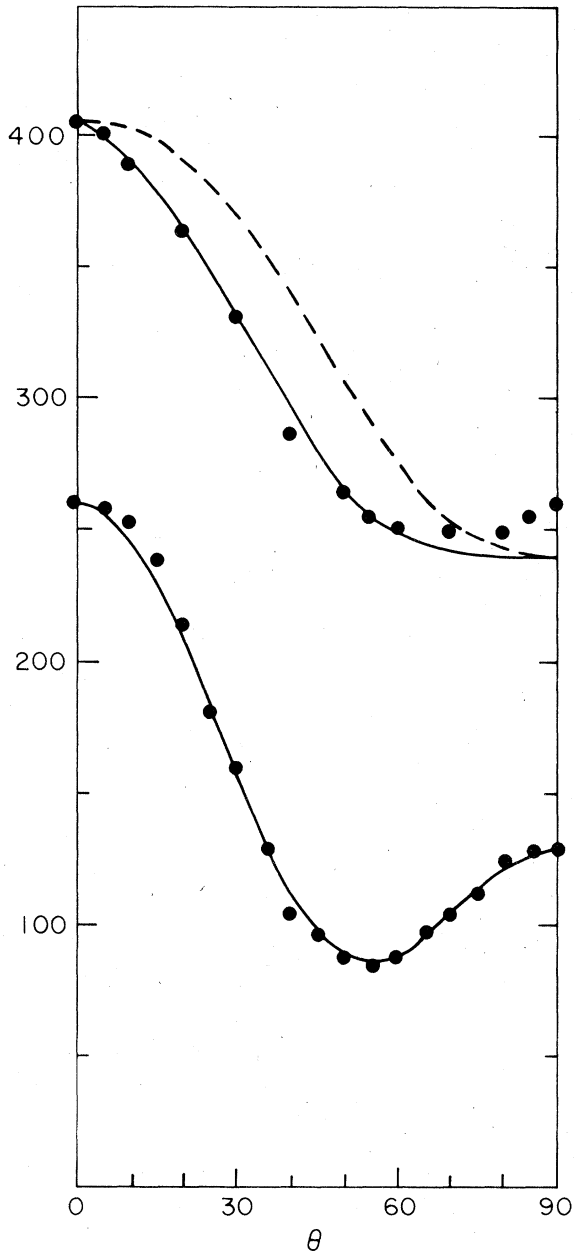

FIG. 5. Anisotropy of the EPR linewidth at $c=0.57$. The lower curve taken at 295 K shows the $(3\cos^2\theta-1)^2$ variation characteristic of long-wavelength spin diffusion in two dimensions. The upper data taken at 20 K follow a $(1+\cos^4\theta)$ anisotropy (solid) curve more closely than the $(1+\cos^2\theta)$ (dashed) curve expected for isotropic AF fluctuations.

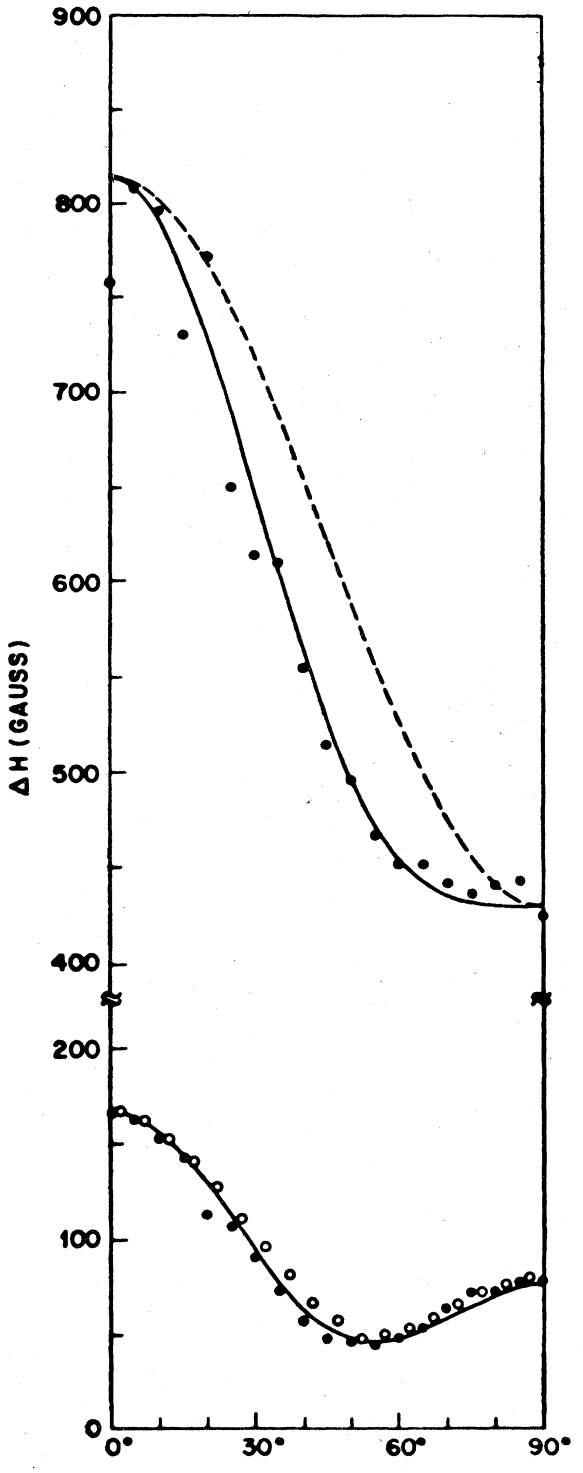

FIG. 6. Linewidth anisotropy above the percolation limit, $c=0.7$. The lower 295-K data points were taken at 35 (solid) and 17.4 GHz (open). The upper 23-K data follow $(1+\cos^4\theta)$ rather than $(1+\cos^2\theta)$, as in Fig. 5, despite the proximity to AF ordering.

The linewidth anisotropy measured at room temperature for a sample with $c = 0.57$ is shown in the lower part of Fig. 5. The solid curve corresponds to

$$\Delta H(\theta) = 85 + 44(3\cos^2\theta - 1)^2 \text{ G} \qquad (14)$$

and clearly is an excellent fit. The same functional variation is observed at both higher and lower concentrations (Fig. 6 for $c = 0.70$, and Fig. 7 for $c = 0.30$). The extremal linewidths measured at room temperature in the principal orientations $\theta = 0°$, 55°, and 90°, with samples of nine different nominal concentrations, as well as data for pure K_2MnF_4 are shown in Fig. 8. It is evident that the 0° and 90° linewidths increase rapidly at concentrations near and below the percolation threshold, $c_p = 0.59$. In contrast, at the "magic" angle, $\theta = 55°$, where $3\cos^2\theta - 1 = 0$ the linewidth varies only moderately as

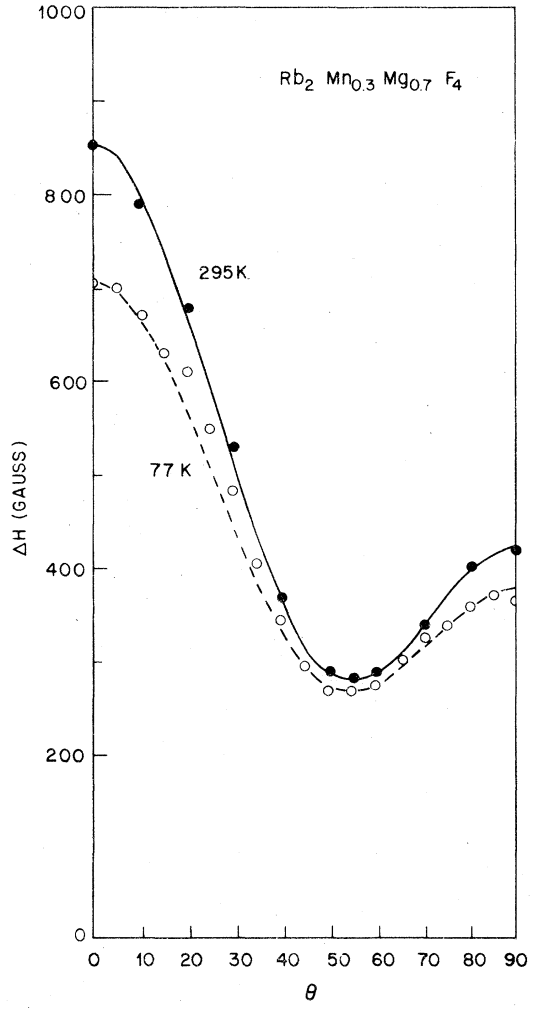

FIG. 7. Linewidth anisotropy at 295 and 77 K for a $c = 0.3$ sample well below percolation. Even with small clusters the $(3\cos^2\theta - 1)^2$ variation persists.

c passes through c_p. The latter point is not consistent with the data reported by Takano and Yokogawa for $K_2Mn_cMg_{1-c}F_4$, though their study does also show the rapid rise of $\Delta H(0°)$ and $\Delta H(90°)$ as c decreases through c_p.[6]

The horizontal error bars indicated in Fig. 8 correspond to the ± 4% concentration ranges observed over entire boules in the neutron investigations.[1] The strong variation of $\Delta H(0°)$ for $c \lesssim c_p$ suggests that the ESR linewidth could be used as a very sensitive indicator of concentration if a few precise calibrations could be established by chemical analysis of the ESR samples. This extreme sensitivity of linewidth to concentration near percolation revealed the weak radial concentration gradient within a cleavage slice mentioned above.

As the temperature is reduced below room temperature the parallel and perpendicular linewidths decrease markedly, the $(3\cos^2\theta - 1)^2$ anisotropy persisting down to ~60 K and below. The linewidth at $\theta = 55°$ which measures the isotropic background [α

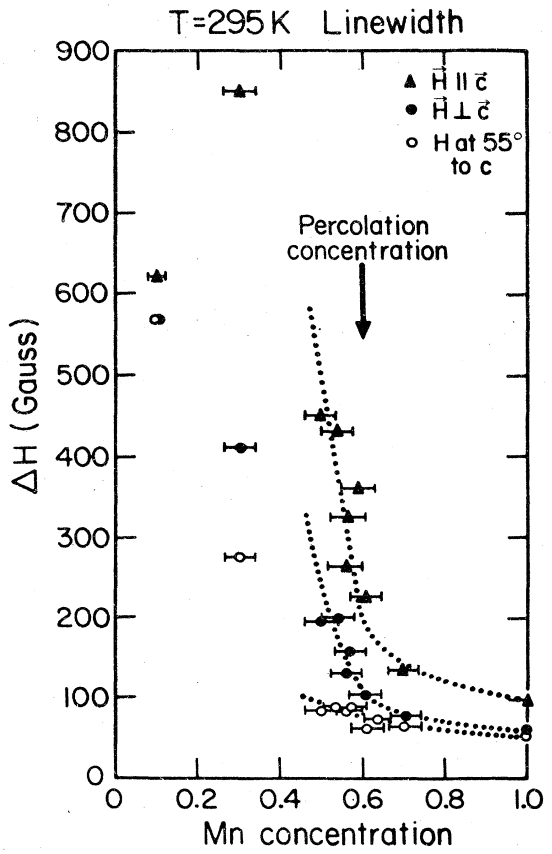

FIG. 8. Extremal linewidths vs concentration at room temperature. The rapid divergence of the parallel and perpendicular linewidths as c decreases through $c_p = 0.59$ reflects the inhibition of long-wavelength spin diffusion as the percolation lattice breaks up into finite clusters.

term in Eq. (7)] changes very little upon cooling but does decrease slightly. These effects are shown for the principal orientations in samples of three concentrations spanning the percolation concentration ($c=0.70$, Fig. 9; $c=0.61$, Fig. 10; and $c=0.54$, Fig. 11).

At lower temperatures, i.e., $T<60$–30 K, all linewidths increase very rapidly—note the logarithmic temperature scales of Figs. 9–11— and the anisotropy changes. The latter point is most clearly seen in the upper portions of Figs. 5 and 6. At 20 K the $c=0.57$ sample shows an anisotropy which does not follow the $(1+\cos^2\theta)$ variation expected for isotropic AF fluctuations. A reasonably satisfactory fit is provided if we take $f(\theta)=1+\cos^4\theta$, however, and the deduced isotropic background term is still quite near its room-temperature value [see Eq. (14)]

$$\Delta H(\theta)=80+160(1+\cos^4\theta)\ \text{G}\ . \qquad (15)$$

Since no true long-range order can develop below the percolation threshold one might suspect that the unexpected anisotropy is explicitly related to the absence of an ordering temperature, particularly since it is already known that the idealized $(1+\cos^2\theta)$ behavior is accurately followed in pure K_2MnF_4.[15]

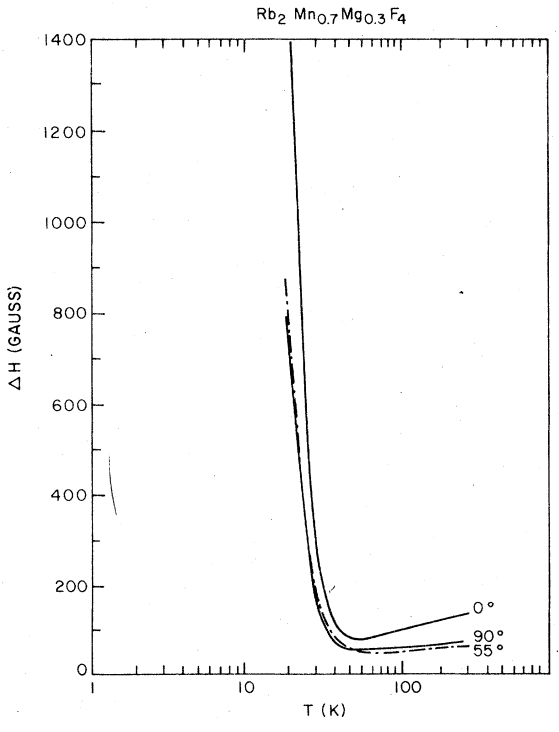

FIG. 9. Linewidths in the three principal orientations vs $\log_{10}T$ for $c=0.70$. The high-temperature dipolar contribution is weak whereas the low-temperature AF-correlation contribution is divergent due to the onset of long-range order at ~ 15 K.

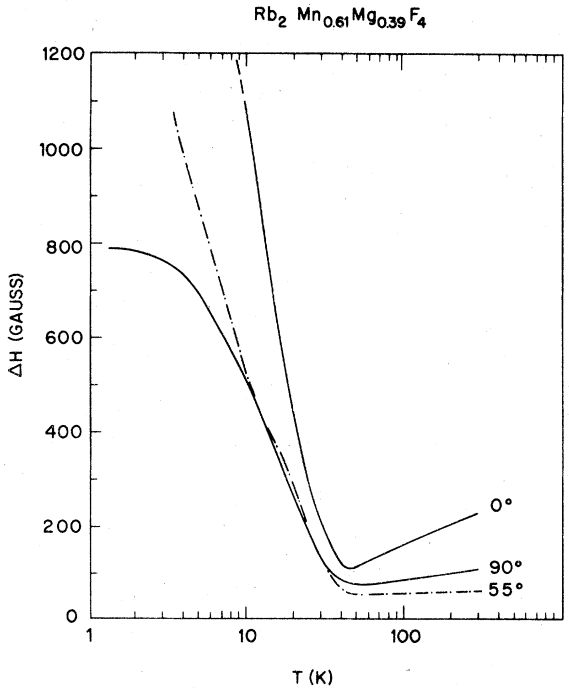

FIG. 10. Principal linewidths vs $\log_{10}T$ for $c=0.61$, near c_p. The dipolar contribution increases relative to Fig. 9 and the low-temperature rise is weaker. Note the saturation of $\Delta H(90°)$ at the lowest temperatures.

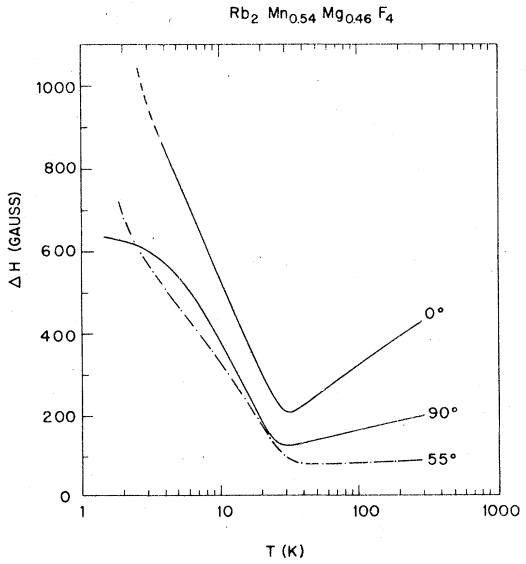

FIG. 11. Principal linewidths vs $\log_{10}T$ for $c=0.54$ below c_p. The dipolar contribution is now very strong and the low-temperature rise much weaker. No evidence of long-range order is observed even at the lowest temperature.

That this is not the case is seen in Fig. 6 for $c=0.70$ where an anisotropy run at 23 K is well described by

$$\Delta H(\theta)=45+385(1+\cos^4\theta)\ \text{G} \tag{16}$$

and the rapid linewidth divergence displayed by this sample at still lower temperatures (Fig. 9) clearly indicates long-range order does occur near 15 K, the resonance having become almost unobservably broad and shifted from the $g=2$ position as the anisotropy and exchange fields develop. This estimated ordering temperature is somewhat higher than the 11-K value expected for $c=0.70$ on the basis of the susceptibility studies by Breed *et al.*[16] of the $K_2Mn_cMg_{1-c}F_4$ alloy series but the two temperatures are compatible within the uncertainty in the concentration. The $(1+\cos^4\theta)$ anisotropy does, therefore, appear to be characteristic of the rising linewidth, low-temperature regime of samples near the percolation concentration without regard to the presence or absence of true ordering but it surely does originate from the growth of short-range AF correlations. It is thus reasonable to examine the data for evidence of critical, i.e., power-law behavior. Figure 12 is a log-log plot of the linewidth at 55°, where any residual dipolar contribution vanishes, with the background contribution ($\Delta H_{\min}$) subtracted for two concentrations near the percolation threshold. The high-temperature ends of these curves are necessarily imprecise for values of $\Delta H_{55}-\Delta H_{\min}\lesssim 10$ G due to the subtraction. Conversely much above 100 G there is clearly a tendency toward saturation. We show as the dashed line in Fig. 12 the idealized exponent of -4.5 for the theory with crossover exponent $\phi=1$. It is clear that the rapid increase in the critical part of the linewidth is approximately consistent with this. However, there is no temperature subregion where one can realistically describe the linewidth divergence by a simple power law in T. Rather, spin-space crossover and saturation effects appear to fundamentally alter this idealized behavior. Clearly, a better theory is required; we hope that these experiments will serve to stimulate such calculations.

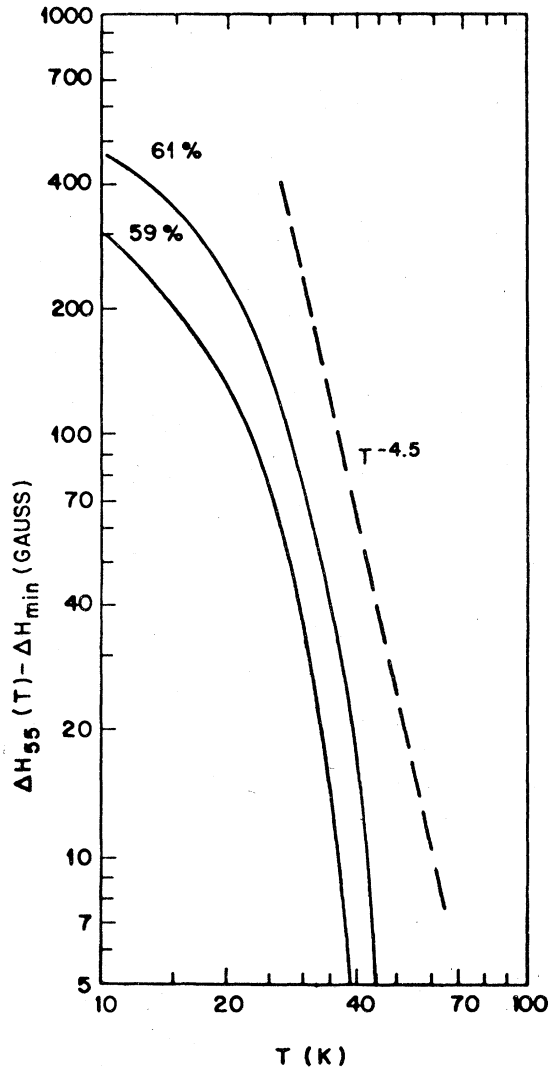

FIG. 12. Log-log plot of $\Delta H(55°)$ with the background, $\Delta H_{\min}$, subtracted to reveal any evidence of critical behavior. The dashed line ($T^{-4.5}$) is expected from theoretical considerations if the concentration-temperature crossover exponent $\phi=1$.

The contrasting temperature variations of the dipolar ($q=0$) and AF-correlation ($q\sim K_0$) contributions to the linewidth are particularly well displayed by superposing the $\Delta H(0)$ vs T curves for the three concentrations of Figs. 9–11, spanning c_p, as shown in Fig. 13. The rapid decrease of the spin diffusive $q=0$ contribution at high temperatures as c increases through c_p stands in marked contrast to the extremely rapid increase of the AF-fluctuation contribution at the low-temperature end as long-range order appears above c_p.

We note that for the $c=0.70$ sample no $g=2$ resonance signal is observable below 15 K. On the other hand for the $c=0.61$ sample one sees a narrow Lorentzian resonance line down to 1.65 K for the $\theta=90°$ geometry. A very much broader, structured line is observed for $\theta=0°$. Neutron scattering measurements on a sample from the $c=0.61$ boule show a well-defined 2-D AF transition at 8 K. The rapid rise of the $\theta=0$ linewidth which we observe near 8 K is consistent with this result. However, in contrast to the $c=0.70$ sample a strong $g=2$ EPR line is still observable in the long-range-ordered state. This apparently anomalous result may be understood from the percolation-cluster statistics. As is evident from Fig. 13, for $c\simeq 0.61$ a significant percentage of the spins are located in clusters which are disconnected from the infinite network. These clusters will remain paramagnetic down to the lowest temperatures, and hence they will give a strong EPR signal even in the

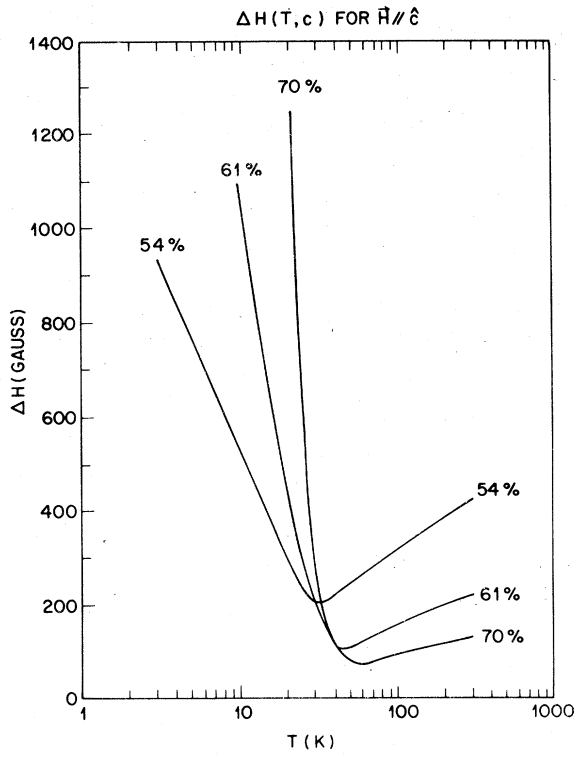

FIG. 13. $\Delta H(0°)$ vs $\log_{10} T$ curves from Figs. 9–11 superposed to display the rapid decrease of the high-temperature dipolar contribution as c increases through c_p and the concomitant rapid increase of the low-temperature AF-correlation contribution as long-range order appears.

presence of long-range order. For $c = 0.70$, on the other hand, very few of the spins belong to isolated clusters and accordingly one expects a much weaker resonance line.

Finally we shall describe two phenomena which occur only at the lowest temperatures attained in these experiments (~ 1.6 K) and in the concentration range very near the percolation threshold. Both effects are the results of inhomogeneous internal magnetic field distributions which we believe reflect critical slowing of spin fluctuations as we approach $T = 0$ for $c < c_p$.

The first is a gross line-shape distortion which is barely notable in the absorption-derivative spectra but is readily observable when absorption is directly recorded, as shown in Fig. 14 for $c = 0.59$ observed at 35 GHz. At 4.2 K most of the absorption intensity still lies in the resonance peak centered at $g = 2$, though some asymmetry is seen, particularly for $\vec{H} \| \hat{c}$. The distortion is much stronger at 1.6 K where roughly half the total absorption has shifted to lower magnetic fields in all orientations and even appears to form a very broad but resolved peak for $\vec{H} \| \hat{c}$. It is clear that the spins are no longer able to resonate in a homogeneous Lorentzian (exchange-narrowed) line. One is tempted to attribute the effect to nonstatistical concentration gradients leading to "local long-range order", i.e., regions where $c > c_p$ which have a distribution of small but finite ordering temperatures in the range 5 K and below with anisotropy and exchange fields which cause the net moment in those regions to be shifted away from $g = 2$. While we have not as yet been able to rule this out completely, the fact that several very small, adjacent samples exhibit very similar spectra seems to imply that the inhomogeneity is not due to nonstatistical effects but, rather, is intrinsic to the percolation regime where the relaxation times of the larger spin clusters with weak magnetic moments must slow arbitrarily upon cooling. This is seen on the time scale of 10^{-10} sec in the neutron experiments; in our EPR experiments, the inhomogeneous line distortion of Fig. 14 implies relaxation times $\gtrsim 10^{-9}$ sec for the larger clusters.

The second, more subtle low-temperature phenomenon indicates a finer scale inhomogeneity of

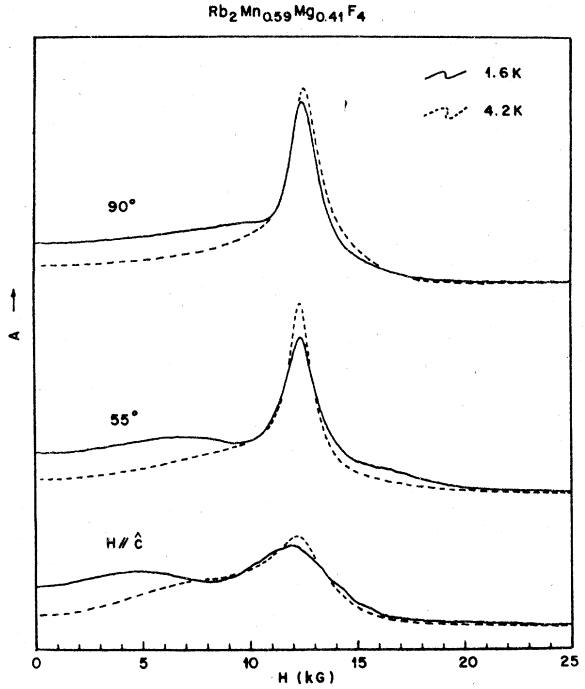

FIG. 14. Absorption spectra taken at 35 GHz with a sample of nominally the percolation concentraion, $c = 0.59$. The dashed curves observed at 4.2 K show some distortion, particularly for $\vec{H} \| \hat{c}$, which becomes very pronounced at 1.6 K. The intensity shifted to fields lower than the $g = 2$ peak is attributed to large clusters whose relaxation times have become $> 10^{-9}$ sec allowing AF anisotropy and exchange fields to become visible.

the internal magnetic field. It is barely visible in Fig. 14 as a weak modulation of the envelope of the $g=2$ peak when $\vec{H}\|\hat{c}$. Such structure is, of course, much more easily observed in the derivative spectrum. Resolution is also improved by decreasing the magnetic concentration somewhat. The most esthetic example found thus far is shown in Fig. 15 for $c=0.54$ where the single $\vec{H}\|\hat{c}$ resonance peak broadens and becomes resolved into a nine-line pattern with roughly triangular intensity ratios at 1.6 K. Because the outermost components are extremely weak it proved easier to study the anisotropy of the pattern at $c=0.57$ as shown in Fig. 16. Starting with a maximum average interval between lines of 1.15 kG for $\vec{H}\|\hat{c}$ the pattern narrows slowly as the field is rotated. The outermost components weaken and then a rather remarkable "collapse" of the multiline pattern into a single resonance occurs for $\theta \gtrsim 60°$. This resonance continues to narrow out to $\theta=90°$ and has a line shape which may be a weak admixture of dispersion with the absorption as can occur when a very intense resonance excessively loads the cavity. It does appear to have a Lorentzian shape characteristic of exchange narrowing, however, as will be discussed in Sec. IV. There is also a modest shift of the center of the pattern from 12.5 kG ($g=2$) for $\vec{H}\|\hat{c}$ to 13.1 kG for $\vec{H}\perp\hat{c}$. The shift is opposite to the demagnetizing shift expected for a paramagnetic plate. It most probably is a residual "image" effect. The origin of the nine-line superstructure must lie in the statistical distribution of nearly static local magnetic fields experienced by magnetic moments which are otherwise free, i.e., not part of slowing clusters since the center of the pattern remains at $g=2$ (save for the "image" shift). The implication of unpaired spins or small clusters with net moments (ferrimagnetic clusters are discussed by Harris and Kirkpatrick[4]) suggests counting these nearly isolated entities.

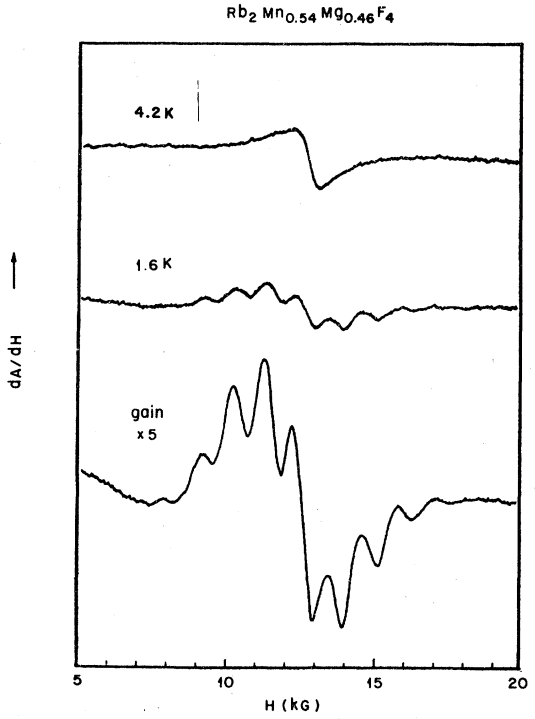

FIG. 15. Derivative spectra for $\vec{H}\|\hat{c}$ of a sample below but near the percolation concentration ($c=0.54$) showing the sudden broadening into a fine-structure pattern which occurs upon cooling from 4.2 to 1.6 K. The lowest trace taken at increased gain fully reveals the nine-line pattern.

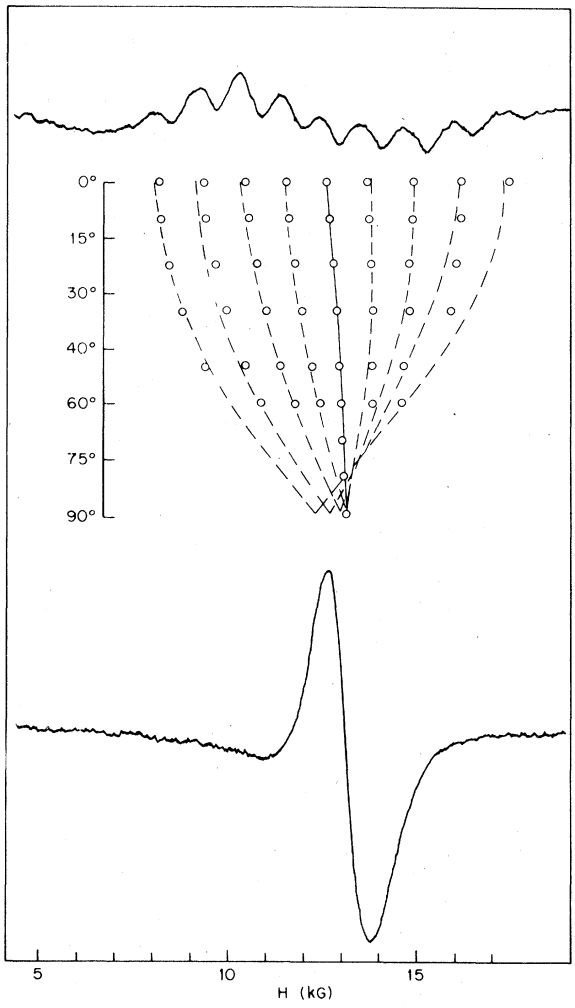

FIG. 16. Anisotropy of the nine-line fine structure observed at the lowest temperatures in samples near the percolation threshold ($c=0.57, T=1.6$ K, 35 GHz). The solid curve is drawn in to establish an empirical centroid. The dashed curves are calculated displacements of the fine-structure components assuming the local magnetic fields are locked to the $\hat{c}$ axis as the applied field is rotated. Beyond $\theta \sim 60°$ only a single reconance line is observed, suggesting a marked anisotropy of the fluctuation spectrum.

At percolation 2.8% of the spins are isolated in the sense that all *nearest* neighbors are nonmagnetic. Since there are four *next*-nearest-neighbor sites a set of nine discrete magnetic field values will result if any magnetic next-nearest neighbor can have its moment only "up" or "down". The latter assumption is, in fact, plausible since such next-nearest neighbors are very likely to be attached to a large (slow) cluster by one or two AF nearest-neighbor couplings (see Fig. 2). Such a mechanism would lead to an approximate intensity-ratio pattern of 1:5:15:26:31:26:15:5:1 which is qualitatively consistent with Fig. 15. The anisotropy is also crudely consistent with such a distribution of local magnetic fields locked along the $\hat{c}$ axis as indicated in Fig. 16. We favor this explanation of the nine-line superstructure and shall discuss it further in Sec. IV.

It is, however, useful to note that higher-order isolated clusters are rare: At percolation 0.16% of all spins form right-angle nearest-neighbor triples with five available next-nearest-neighbor sites; 0.033% of all spins form linear nn triples with four available nnn sites. While these and still higher-order ferrimagnetic clusters will occur and contribute some intensity to the resonance at $g=2$ it is very likely that the net result is a relatively unstructured background on which is superposed the nine-line pattern due to isolated spins. Careful examination of the observed spectra reveals subtle but reproducible substructure which presumably results from the higher-order isolated clusters. This substructure implies that the fluctuation times must be longer than 10^{-8} sec for $\vec{H}\|\hat{c}$.

IV. DISCUSSION

It is evident that the EPR of these dilute two-dimensional antiferromagnets exhibits richly detailed behavior as a function of concentration, temperature, and magnetic field direction. Certain qualitative features are consistent with our expectations based on the simple theory outlined in Sec. II but several unanticipated effects have been observed. The physical significance of the experimental results will now be discussed in somewhat more detail.

Consider first the results at room temperature where Figs. 5–7 show that the linewidth contribution due to spin diffusion $\beta(T)(3\cos^2\theta-1)^2$, dominates the high-temperature regime from $c=0.30$ to $c=1$. The most striking variation occurs near and below the percolation concentration $c\approx c_p=0.59$. From Fig. 8 it is clear that the background term, $\alpha(T)$ in Eq. (7) (given by the $\theta=55°$ linewidth) depends only weakly on concentration down to $c=0.50$ and, in particular, shows no marked variation near c_p. In contrast the linewidths at 0° and 90° which reflect $\beta(T)$ increase strongly as the concentration decreases below the percolation value. This drastic increase in β near c_p directly reflects the progressive ramification and breakup of the percolation network. Physically it means that the time for a spin deviation to diffuse away from a given site becomes longer and longer as the network breaks up. Indeed, for $c<c_p$ where all clusters are finite a spin deviation never completely leaves a given cluster. A similar effect has previously been observed by Richards in an impure one-dimensional antiferromagnet[17]; in that case the percolation concentration can be taken as $c_p=1$.

As shown in Figs. 9–11 the diffusive component $\beta(T)(3\cos^2\theta-1)^2$ continues to contribute significantly to ΔH in the various samples down to fairly low temperatures. The coefficient β decreases approximately linearly with decreasing temperature consistent with the qualitative argument given in Sec. II. On the other hand the background contribution $[\Delta H(55°)]$ is very nearly temperature independent whereas a moderate increase with decreasing temperature was anticipated. The observed behavior is consistent with that of the fully concentrated system which appears to be predicted by the more detailed calculations of Richards and Salamon.[5]

Further cooling brings about a reversal in the linewidth variation which defines the onset of a distinct low-temperature regime. In the pure material $d(\Delta H)/dT$ changes sign at ~ 80 K and ΔH ultimately diverges at the Néel temperature 38.4 K. As shown in Fig. 9 for $Rb_2Mn_{0.7}Mg_{0.3}F_4$ the slope reversal occurs near 60 K and, as noted earlier, ΔH diverges at ~ 18 K. The reduction in characteristic temperature in the $c=0.70$ sample is, of course, a direct consequence of the magnetic dilution.[16] In samples near the percolation threshold $d(\Delta H)/dT$ changes sign at ~ 45 K signaling the onset of AF correlations in the percolation clusters and the consequent appearance of the $\gamma(T)f(\theta)$ term of Eq. (7). However, as noted previously no true AF gap develops and, for $\vec{H}\|\hat{c}$, an exchange-narrowed resonance centered at $g=2$ is observed down to 1.6 K. Hence the percolation threshold with its attendant loss of long-range order manifests itself as directly in the ESR spectra as it did in the neuron scattering experiments.

The detailed temperature and angular dependences of the resonance linewidth in the low-temperature regime for samples near the percolation concentration are of interest as they contrast with the behavior of the pure material. In Fig. 10 it is evident that a "precritical" regime exists in the temperature interval 40 K down to ~ 10 K. Here the ratio $\Delta H(0°)/\Delta H(90°)\simeq 2$ after subtracting off a presumed isotropic background contribution of ~ 60 G extrapolated from the α term $[\Delta H(55°)]$ above 50 K. This value of $\Delta H(0°)/\Delta H(90°)$ is expected on the basis of the theory outlined in Sec. II but the predicted $(1+\cos^2\theta)$ anisotropy is not observed. Instead we find $f(\theta)\simeq 1+\cos^4\theta$ to be a better fit to the data. Similarly the temperature dependence is quali-

tatively as expected, i.e., a rapid increase of $\gamma(T)$ with decreasing temperature but the predicted $T^{-4.5}$ behavior expected for the crossover exponent $\phi=1$ is not quantitatively borne out by the experiments, no simple power law occurring in Fig. 12. Clearly the theory of Sec. II needs extension to describe the percolation regime. In particular we feel that the assumption of isotropic spin fluctuations is a weak one since the detailed neutron studies[9] and the lowest-temperature ESR spectra (to be discussed) clearly indicate that the longitudinal fluctuations along $\hat{c}$ slow much more than the transverse fluctuations. Nevertheless, we believe that the basic physical picture of a rapidly increasing ΔH at low temperatures arising from the combined effects of growing AF correlations between neighboring spins and critical slowing down of the cluster spin dynamics must be correct near percolation as it is in the precritical regime of the more concentrated 2-D AF crystals.

Finally there is a lowest-temperature regime in the samples near percolation as seen in Figs. 10 and 11. Below ~ 10 K the rapid increase of ΔH versus decreasing temperature goes over into a saturated limit with the striking fine structure and anisotropy of Figs. 15 and 16 becoming visible at 1.6 K. The contrast between the multiline spectrum seen for $\vec{H}\|\hat{c}$ versus the exchange-narrowed single resonance for $\vec{H}\perp\hat{c}$ (Fig. 16) is clear evidence for the anisotropic fluctuations suggested above. Whereas a model with next-nearest-neighbor spins producing roughly static local magnetic fields locked along $\hat{c}$ at the site of "nearly isolated" spins appears to be a fair description of the multiline spectra seen from magnet orientations along $\hat{c}$ out to $\sim 60°$, the collapse of the spectrum into a single homogeneous line at larger angles implies a change in the spin fluctuation time from $\gtrsim 10^{-8}$ sec along $\hat{c}$ to $\lesssim 3\times 10^{-10}$ sec perpendicular to $\hat{c}$.

The magnitude of the splittings in the nine-line lowest-temperature spectrum is of interest in the context of the proposed origin of these magnetic fields. The splitting does not appear to depend on concentration over the narrow range near the percolation threshold where the spectrum is observed. The spacing of the lines averages ~ 1150 G, close to but definitely larger than the nearest-neighbor dipolar interaction of 973 G. As mentioned in Sec. III, there may be a variety of possible explanations of the multiline spectrum but we favor the quasi-isolated spin subject to next-nearest-neighbor interactions. The most important physical implication is independent of any particular model, however, i.e., that the large clusters are frozen on a time scale of $\sim 10^{-8}$ sec since reproducible substructure on a field scale of ~ 10 G is observed.

Consider the computer-generated percolation array of Fig. 2. The site probability of nearly isolated spins in the sense of having no magnetic nearest-neighbor ions is 1.67% at $c=0.59$. In the frozen limit we may write the effective Hamiltonian for these spins as

$$H=g\mu_B\vec{H}\cdot\vec{S}+\sum_{\text{occupied nnn}}\left(J_{\text{nnn}}+\frac{3g^2\mu_B^2}{2r_{\text{nnn}}^3}\right)\times S^z\langle S^z_{\text{nnn}}\rangle+\cdots, \tag{17}$$

where the dots stand for more-distant-neighbor dipolar fields. Dipolar sums in the fully concentrated lattice show that the dipolar fields from spins beyond nnn average nearly to zero so we will ignore the more-distant-neighbor contribution. Now, depending on the occupation numbers, each nearly isolated spin may have between 0 and 4 magnetically occupied nnn sites. Further, these nnn spins "locked" to slow or static clusters may be either parallel or antiparallel to $\hat{c}$ so that $\langle S^z_{\text{nnn}}\rangle=\pm(\frac{5}{2}-\Delta_0)$ where Δ_0 is the zero-point spin deviation. Hence, we expect nine lines centered on the $g=2$ resonance field with an interline spacing

$$\delta H=\frac{\langle S^z_{\text{nnn}}\rangle}{g\mu_B}\left(J_{\text{nnn}}+\frac{2g^2\mu_B^2}{2r_{\text{nnn}}^3}\right). \tag{18}$$

If $\Delta_o=0$ the dipolar contribution $15\,g\mu_B/4r^3_{\text{nnn}}=334$ G and the exchange contribution is deduced to be $J_{\text{nnn}}=0.0037$ meV assuming AF nnn exchange as in pure Rb_2MnF_4. This value is much smaller than $J_{\text{nnn}}=0.012$ meV deduced from the neutron scattering studies of the fully concentrated material. A possible cause of reduction of δH in the diluted samples could be the zero-point spin deviation Δ_0 but in both K_2MnF_4 and Rb_2MnF_4 Walstedt *et al.*[18] found $\Delta_0=0.17$ or 6.8%. While it is expected that the zero-point deviation will be appreciably larger for the nnn spins considered here since they are only attached to their clusters by one or two bonds, it is unreasonable to attribute all the reduction of δH to this cause since $\Delta_0=0.17$ or 68% would be required. A far more likely explanation is that J_{nnn} is indeed considerably reduced in the dilute material since the nnn superexchange linkages must proceed via nonmagnetic Mg^{2+} ions, rather than Mn^{2+} ions, in the case of the nearly isolated spins. Thus, despite numerical discrepancy, we feel that this class of spins is the most likely source of the observed nine-line "frozen cluster" spectrum.

A second, although less likely, origin of the multiline resonances is the "ferrimagnetic" configurations noted by Harris and Kirkpatrick.[4] Again, as is evident, in Fig. 2, the majority of clusters have a net spin which is nonzero. Indeed for $c>c_p$, Harris and Kirkpatrick have suggested that the low-temperature susceptibility and hence the resonance signal will be dominated by such clusters. These finite-spin clusters will also exhibit a resonance centered about $g=2$, with a width, in the simplest picture,

corresponding to the average anisotropy field seen by the individual spins in the cluster. This anisotropy field is dominated by the nn dipolar interaction which has a value of 973 G per nn. It may be possible that the cluster resonance in the frozen limit would also be quantized in these units thence giving rise to an apparent multiline spectrum. Of course, 973 G is rather less than the actual spacing of 1100 G and we cannot account for this difference. This would seem to mitigate against such an explanation. In any case, a proper theoretical treatment of the "ferrimagnetic cluster" resonance properties would be most valuable.

Finally, the absorption observed at lower fields (cf. Fig. 8) most likely corresponds to a pseudo-antiferromagnetic resonance mode arising from the zero-spin and possibly also the finite-spin clusters.

V. FINAL REMARKS

It is evident that the EPR spectra do indeed exhibit rather complex behavior in these samples and that they may yield suprisingly detailed information about the spin dynamics and antiferromagnetic correlations in the percolation regime. In particular, we have shown that by a careful consideration of each of the temperature dependence, angular variation, and concentration dependence of the resonance widths one can isolate the $\vec{q} \simeq 0$, $\vec{q} \simeq \vec{K}_0$, and general $\vec{q}$ dynamical proccesses. Our results in the system $Rb_2Mn_cMg_{1-c}F_4$ are, in general, consistent with both our current picture of percolation in these materials and with the theory of EPR in 2-D antiferromagnets. They demonstrate, in turn, that EPR may be used as an effective probe of percolation in other systems where rather less information is available. There are, of course, many detailed and quite interesting results which we either do not understand or for which we have only been able to offer qualitative explanations. The most important of these is the behavior at very low temperatures in the $c \simeq c_p$ samples. A theory for EPR in this "frozen cluster" regime would be most welcome.

ACKNOWLEDGMENTS

We should like to thank W. F. Brinkman, L. R. Walker, and R. E. Walstedt for extended and most valuable discussions. We should also like to thank R. A. Cowley, S. Geschwind, and Professor V. Jaccarino for helpful comments. The assistance of A. L. Simons in the computer studies is greatly appreciated. The work at MIT was supported by the NSF Materials Research Laboratory Grant No. DMR-76-80895.

[1]R. J. Birgeneau, R. A. Cowley, G. Shirane, and H. J. Guggenheim, Phys. Rev. Lett. 37, 940 (1976).
[2]R. A. Cowley, R. J. Birgeneau, G. Shirane, and E. C. Svensson, Phys. Rev. Lett. 39, 894 (1977).
[3]P. L. Leath, Phys. Rev. Lett. 36, 921 (1976); S. Kirkpatrick, Phys. Rev. Lett. 36, 69 (1976).
[4]A. B. Harris and S. Kirkpatrick, Phys. Rev. B 16, 542 (1977).
[5]P. M. Richards and M. B. Salamon, Phys. Rev. B 9, 32 (1974).
[6]H. Takano and Y. Yokozawa, J. Phys. Soc. Jpn. Lett. 42, 1059 (1977).
[7]R. A. Cowley, G. Shirane, R. J. Birgeneau, and H. J. Guggenheim, Phys. Rev. B 15, 4292 (1977).
[8]R. J. Birgeneau, H. J. Guggenheim, and G. Shirane, Phys. Rev. B 1, 2211 (1970).
[9]R. J. Birgeneau, R. A. Cowley, G. Shirane, J. A. Tarvin, and H. J. Guggenheim (unpublished).
[10]D. L. Huber, Phys. Rev. B 6, 3180 (1972); J. Phys. Chem. Solids 32, 2145 (1971).
[11]H. Mori and K. Kawasaki, Prog. Theor. Phys. 27, 529 (1962); 28, 971 (1962); K. Kawasaki, Prog. Theor. Phys. 39, 285 (1968).
[12]M. H. Seehra and D. L. Huber, in *Proceedings of the 20th Conference on Magnetism and Magnetic Materials, 1974, San Francisco,* edited by C. D. Graham, Jr., G. H. Lander, and J. J. Rhyne, AIP Conf. Proc. No. 24 (AIP, New York, 1975), p. 261.
[13]B. I. Halperin and P. C. Hohenberg, Phys. Rev. 177, 952 (1969).
[14]D. Stauffer, Z. Phys. 1322, 161 (1975); H. E. Stanley, R. J. Birgeneau, P. J. Reynolds, and J. F. Nicoll, J. Phys. C 9, L553 (1976); T. C. Lubensky, Phys. Rev. B 15, 311 (1977); M. J. Stephen and G. S. Grest, Phys. Rev. Lett. 38, 567 (1977).
[15]H. W. de Wijn, L. R. Walker, J. L. Davis, and H. J. Guggenheim, Solid State Commun. 11, 803 (1972).
[16]D. J. Breed, K. Gilijamse, J. W. E. Sterkenburg, and A. R. Miedema, J. Appl. Phys. 41, 1267 (1970).
[17]P. M. Richards, Phys. Rev. B 10, 805 (1974).
[18]R. E. Walstedt, H. W. de Wijn, and H. J. Guggenheim, Phys. Rev. Lett. 25, 1119 (1970).